nature medicine

Chronic stress promotes tumor growth and angiogenesis in a mouse model of ovarian carcinoma

Premal H Thaker[1,10], Liz Y Han[1,10], Aparna A Kamat[1,10], Jesusa M Arevalo[2], Rie Takahashi[2], Chunhua Lu[1], Nicholas B Jennings[1], Guillermo Armaiz-Pena[1], James A Bankson[3], Murali Ravoori[4], William M Merritt[1], Yvonne G Lin[1], Lingegowda S Mangala[1], Tae Jin Kim[1], Robert L Coleman[1], Charles N Landen[1], Yang Li[1], Edward Felix[5], Angela M Sanguino[6], Robert A Newman[5], Mary Lloyd[7], David M Gershenson[1], Vikas Kundra[4,8], Gabriel Lopez-Berestein[6], Susan K Lutgendorf[9], Steven W Cole[2] & Anil K Sood[1,7]

Stress can alter immunological, neurochemical and endocrinological functions, but its role in cancer progression is not well understood. Here, we show that chronic behavioral stress results in higher levels of tissue catecholamines, greater tumor burden and more invasive growth of ovarian carcinoma cells in an orthotopic mouse model. These effects are mediated primarily through activation of the tumor cell cyclic AMP (cAMP)–protein kinase A (PKA) signaling pathway by the β_2 adrenergic receptor (encoded by *ADRB2*). Tumors in stressed animals showed markedly increased vascularization and enhanced expression of VEGF, MMP2 and MMP9, and we found that angiogenic processes mediated the effects of stress on tumor growth *in vivo*. These data identify β-adrenergic activation of the cAMP–PKA signaling pathway as a major mechanism by which behavioral stress can enhance tumor angiogenesis *in vivo* and thereby promote malignant cell growth. These data also suggest that blocking ADRB-mediated angiogenesis could have therapeutic implications for the management of ovarian cancer.

Epidemiologic and experimental animal studies have shown that stress may alter tumor growth[1–5]. However, the biological mechanisms underlying such effects are not well understood, and their clinical significance for human disease remains controversial as a result. Data from animal models suggest that stress can modulate the growth of certain tumors via neuroendocrine regulation of the immune response to tumor cells[1]. However, the uncertain role of the immune system in controlling solid tumors led us to consider an alternative hypothesis: stress mediators from the sympathetic nervous system might directly modulate the growth and malignant behavior of tumor cells, independent of effects on the immune system. Based on our prior studies linking behavioral factors to circulating VEGF levels *in vivo* and showing catecholamine regulation of tumor cell VEGF production *in vitro*[6,7], we sought to determine whether sympathetic nervous system activity might mediate a causal effect of stress on the growth and metastasis of ovarian cancer *in vivo*. We also sought to define the role of angiogenic cytokines in mediating those effects.

These studies used an established orthotopic mouse model in which human ovarian carcinoma cells are inoculated into the peritoneal cavity of nude mice[8]. We then experimentally stressed animals with a new physical restraint system that we designed, in which periodic immobilization induces high levels of hypothalamic-pituitary-adrenal and sympathetic nervous system activity characteristic of chronic stress (**Supplementary Fig. 1** online). We first examined the effects of stress on tumor growth and metastasis of HeyA8 ovarian cancer cells inoculated 7 d after the initiation of stress. In mice receiving 0, 2 or 6 h of immobilization daily for 21 d, the number of tumor nodules increased by 259% in the 2-h stress group ($P = 0.005$, two-tailed Student's *t*-test) and 356% in the 6-h stress group ($P < 0.001$; **Fig. 1a**). Mean tumor weight increased 242% in the 2-h stress group ($P = 0.01$) and 275% in the 6-h group ($P = 0.005$). Tumor growth was confined to the peritoneal cavity in all control mice, but it spread to the parenchyma of the liver or spleen in 50% of stressed mice ($P = 0.01$). The number and weight of tumor nodules did not differ between the 2- and 6-h stress groups. Therefore, we used the 2-h restraint for all subsequent experiments. Additional experiments with the SKOV3ip1 ovarian cancer cell line and the MB-231 orthotopic breast cancer model (**Fig. 1b**) showed that stress effects on tumor growth were evident in a wide range of tumor cell lines (significant differences in mean tumor weight and nodule number, all $P < 0.01$; **Fig. 1b**). Subsequent studies using social isolation as an alternative stressor also showed a 187% increase in tumor weight ($P < 0.01$) and a 255% increase in nodule count ($P < 0.001$) compared with group-housed control animals (**Fig. 1c**). We also documented longitudinal

[1]Department of Gynecologic Oncology, University of Texas (U.T.) M.D. Anderson Cancer Center, 1155 Herman Pressler, Unit 1362, Houston, Texas 77030, USA. [2]Division of Hematology-Oncology, Department of Medicine, 11-934 Factor Building, University of California Los Angeles (UCLA) School of Medicine, Los Angeles, California 90095, USA. [3]Department of Imaging Physics and [4]Department of Experimental Diagnostic Imaging, U.T. M.D. Anderson Cancer Center, 1515 Holcombe Boulevard, Houston, Texas 77030, USA. [5]Department of Experimental Therapeutics, U.T. M.D. Anderson Cancer Center, 8000 El Rio Street, Houston, Texas 77054, USA. [6]Department of Experimental Therapeutics, [7]Department of Cancer Biology and [8]Department of Diagnostic Radiology, U.T. M.D. Anderson Cancer Center, 1515 Holcombe Boulevard, Houston, Texas 77030, USA. [9]Department of Psychology, University of Iowa, E228 Seashore Hall, Iowa City, Iowa 52241, USA. [10]These authors contributed equally to this work. Correspondence should be addressed to A.K.S. (asood@mdanderson.org).

Received 12 April; accepted 21 June; published online 23 July 2006; doi:10.1038/nm1447

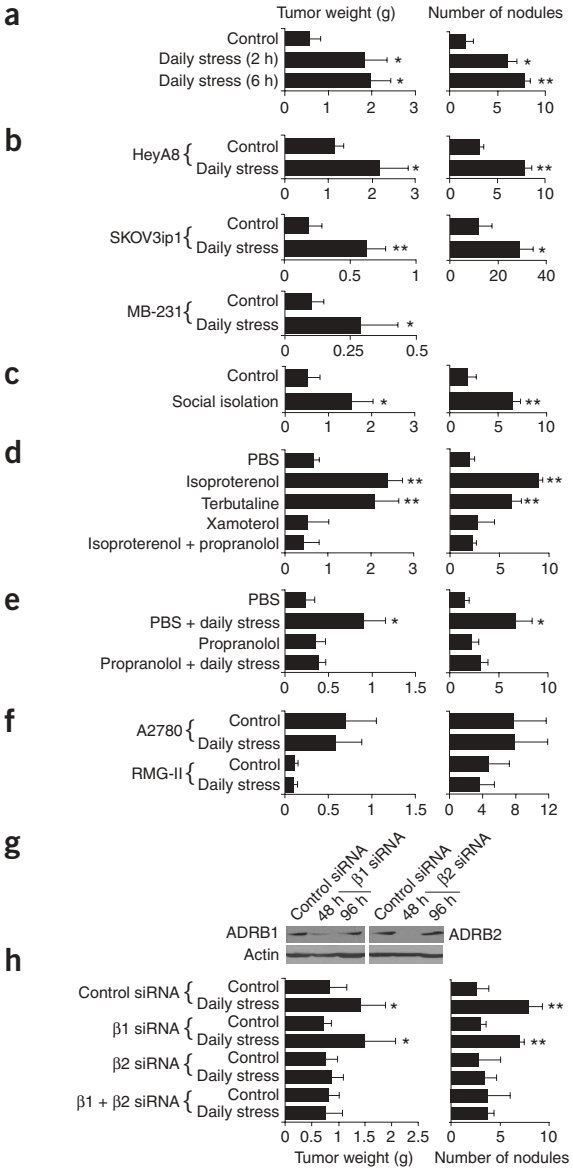

Figure 1 Effect of chronic stress on *in vivo* ovarian cancer growth. (**a**) Quantification of tumor weights and tumor nodules in control mice and in mice stressed for 2 h or 6 h daily that were injected intraperitoneally with HeyA8 ovarian cancer cells. (**b**) Confirmation of the results in mice injected with two different β-adrenoreceptor–positive ovarian cancer cell lines (HeyA8 and SKOV3ip1) intraperitoneally and MB-231 breast cancer cells injected into the mammary fat pad. (**c**) Effects of social isolation stress on the HeyA8 ovarian cancer model. (**d**) The effects of immobilization are mimicked by the chemical stressor isoproterenol (a nonspecific β agonist) and terbutaline (β_2 agonist) but not by xamoterol (β_1 agonist). Mice treated with both isoproterenol plus propranolol (β blocker) have a tumor burden similar to non-stressed mice. (**e**) Propranolol counteracts the effects of chronic stress, confirming the importance of the β-adrenoreceptors. (**f**) Mice injected with β-adrenoreceptor–null ovarian cancer cell lines (A2780 and RMG-II) did not have accelerated tumor growth despite being chronically stressed. (**g**) Western blot of lysate from orthotopic HeyA8 tumors collected 48 h and 96 h after a single dose of siRNA (either control siRNA or siRNA targeted to *ADRB1* (β1) or *ADRB2* (β2)) in DOPC liposomes. The targeted receptors were downregulated. (**h**) Effects of *ADRB1*- and/or *ADRB2*-targeted siRNA on stress-induced *in vivo* HeyA8 tumor growth. Results represent the mean ± s.e.m.; $n = 10$ mice per group. $^*P \leq 0.01$; $^{**}P \leq 0.001$.

development of stress-induced differences in tumor mass using a subcutaneous ovarian cancer model (**Supplementary Fig. 2** online).

To assess the effects of stress on sympatho-adrenal-medullary activity, we measured the size of both adrenal glands[9]. In animals inoculated with HeyA8 cells, the left adrenal gland diameter averaged 1.85 ± 0.25 mm for the control group versus 2.88 ± 0.56 mm for the stressed group ($P = 0.003$, with similar differences noted for right adrenal; data not shown). Based on our previous *in vitro* studies showing expression of β-adrenoreceptors on ovarian cancer cells[7], we performed a series of experiments to evaluate their role in mediating stress effects on tumor growth. Beginning 4 d after tumor cell injection, we treated daily mice bearing HeyA8 ovarian cancer cells with either (i) phosphate-buffered saline (PBS), (ii) 10 mg/kg isoproterenol (a nonspecific β-receptor agonist (hereafter 'β agonist')), (iii) 5 mg/kg terbutaline (a β_2 agonist), (iv) 1 mg/kg xamoterol (a β_1 agonist), or (v) isoproterenol plus 2 mg/kg of the nonspecific β antagonist propranolol. Isoproterenol increased the mean number of tumor nodules by 341% ($P < 0.001$) and the average tumor weight by 266% ($P = 0.001$; **Fig. 1d**). We noted a similar increase in tumor burden with the β_2 agonist terbutaline but not the β_1 agonist xamoterol. Propranolol blocked the isoproterenol-induced increase in tumor growth (**Fig. 1d**), showing that β-adrenergic signaling is essential for that effect. Propranolol also completely blocked the effects of immobilization stress on tumor growth, indicating a critical role for β-adrenergic signaling in behavioral stress effects on tumor growth (**Fig. 1e**). Among stressed animals, we observed invasive disease such as parenchymal metastasis to the liver, spleen, pancreas and diaphragm in 50% of the placebo-treated group, compared with 0% of the propranolol-treated group ($P = 0.01$).

To confirm the relevance of β-adrenergic receptors (encoded by the *ADRB* genes) for stress-induced tumor growth, we screened 17 additional epithelial ovarian cancer cell lines and identified two (A2780 and RMG-II) that were negative for both *ADRB1* and *ADRB2*, as shown by RT-PCR, western blot and lack of intracellular cAMP response to norepinephrine or isoproterenol (data not shown). In contrast to other ovarian cancer cells, stress did not significantly affect tumor weight, number of nodules or the pattern of spread in mice injected with *ADRB1*- and *ADRB2*-negative A2780 or RMG-II cells (**Fig. 1f**). To further define the specific β-adrenergic receptor subtype responsible for stress effects and assess the relative role of host (mouse) versus tumor (human) adrenergic receptors in this model, we used short interfering RNA (siRNA) specific for human *ADRB1* or *ADRB2* to selectively inhibit tumor cell adrenoreceptor expression (**Fig. 1g**). To facilitate *in vivo* distribution, we incorporated the siRNA into a neutral liposome, DOPC[10]. Both control and ADRB1 siRNA-DOPC failed to block stress-induced enhancement of tumor weight and nodules (stress effects continued to be significant at $P < 0.01$), but human ADRB2 siRNA-DOPC efficiently blocked stress-mediated enhancement of tumor cell growth (**Fig. 1h**). Together with data from β-adrenoreceptor–negative cell lines, these results identify ADRB2 receptors on the human tumor cell as the critical mediator of stress effects in this *in vivo* system.

Based on our previous *in vitro* data showing that catecholamines can promote VEGF production by ovarian cancer cells[7], we evaluated the role of angiogenesis in stress effects on *in vivo* tumor growth. In the HeyA8 model, stress significantly enhanced mean vessel density (MVD) counts ($P < 0.001$), and that effect was blocked by the β antagonist propranolol (**Fig. 2a**). We observed similar changes in MVD counts in tumors from non-stressed animals treated with the β agonists isoproterenol or terbutaline, which had significantly higher

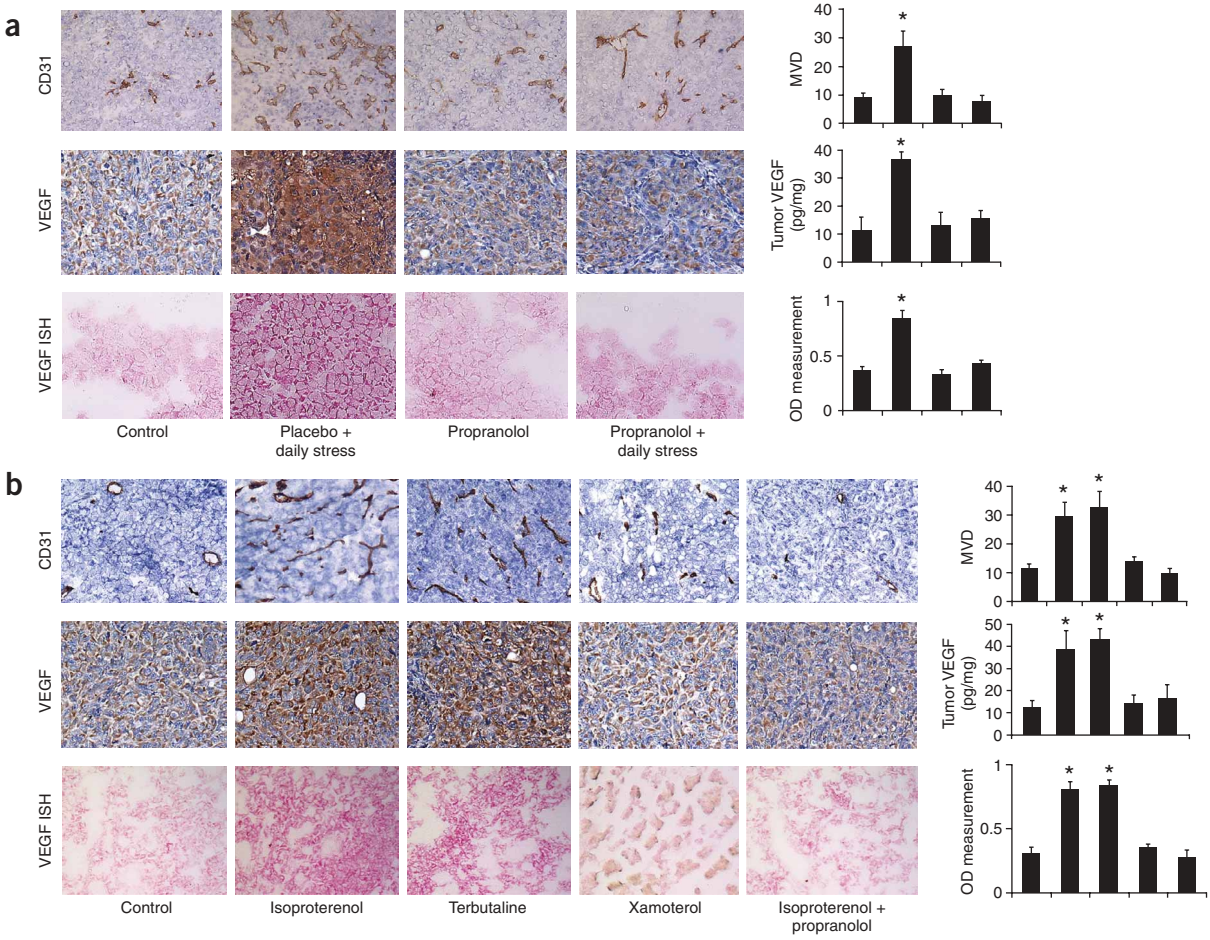

Figure 2 Angiogenesis is increased in chronically stressed animals. (**a**) HeyA8 tumor samples from control and stressed animals treated with placebo or propranolol were stained for VEGF and CD31 (for quantification of mean vessel density (MVD) counts) by immunohistochemistry. We quantified tumor VEGF levels using an ELISA kit. We also stained tumor samples for *VEGF* by *in situ* hybridization (ISH) and calculated optical density (OD) measurements. (**b**) HeyA8 tumor samples from mice treated with a placebo, isoproterenol (nonspecific β agonist), terbutaline (β_2 agonist), xamoterol (β_1 agonist), or isoproterenol plus propranolol were stained for CD31 and VEGF by immunohistochemistry and ISH. We quantified tumor VEGF protein levels by ELISA. MVD was higher in the isoproterenol and terbutaline groups than in controls or in the combination therapy group. All photographs were taken at 200×. The bars in the graphs correspond sequentially to the labeled columns of images at left. Error bars represent s.e.m. $^*P < 0.001$.

MVD counts than did controls ($P < 0.001$); propranolol also blocked those effects (**Fig. 2b**). Stress-induced increases in angiogenesis were accompanied by significant elevation of VEGF protein (as shown by ELISA; $P < 0.001$) and mRNA (as shown by *in situ* hybridization; $P < 0.001$) within tumor tissue (**Fig. 2a**). We observed similar increases in vessel density and VEGF levels in the ADRB-positive MB-231 breast cancer model (**Supplementary Fig. 3** online) and the HeyA8 model with social isolation stress (**Supplementary Fig. 3** online), but not in the *ADRB*-null RMG-II tumors (**Supplementary Fig. 4** online). Immunohistochemistry in the HeyA8 restraint model also demonstrated stress-induced increases in levels of bFGF, MMP-2 and MMP-9 proteins (**Supplementary Fig. 5** online).

We carried out several additional studies to assess more comprehensively the effects of stress on functional and anatomic characteristics of tumor vasculature. In an established Matrigel plug assay (**Fig. 3a**), exogenous VEGF (0.25 nM) enhanced angiogenesis as expected ($P < 0.01$, **Fig. 3b**), and conditioned medium from norepinephrine-treated tumor cells also significantly enhanced angiogenesis ($P < 0.01$) (**Fig. 3a**,**b**). Both catecholamines had modest effects on *in vitro* migration and tube formation of mouse mesenteric endothelial cells[11], but these effects were much smaller than those observed when endothelial cells were exposed to conditioned medium from norepinephrine-treated tumor cells ($P < 0.001$; **Supplementary Fig. 6** online). Consistent with a key mechanistic role of *ADRB* regulation of VEGF, the stimulatory effects of norepinephrine-treated tumor cell conditioned medium was efficiently blocked by PTK787 (inhibits VEGFR2 and other tyrosine kinases) or by pretreatment of tumor cells with propranolol before norepinephrine treatment for collection of conditioned medium (**Supplementary Fig. 6**). These results paralleled confocal microscopy studies showing that tumors from stressed animals contained more tortuous and numerous blood vessels than controls (**Fig. 3c**). This was accompanied by a 24% decrease ($P < 0.01$) in the proportion of blood vessels with pericyte coverage in tumors from stressed animals (**Fig. 3d**), suggesting a more immature vasculature. In addition, *in vivo* magnetic resonance imaging and kinetic analysis showed stress-induced increases in tumor size (**Fig. 3e**) and an increase in the volume transfer constant between plasma and the extravascular extracellular space (K^{trans}, a reflection of flow and permeability; $P < 0.05$; **Fig. 3f**). Tumors from control mice showed a higher return rate constant between the extravascular

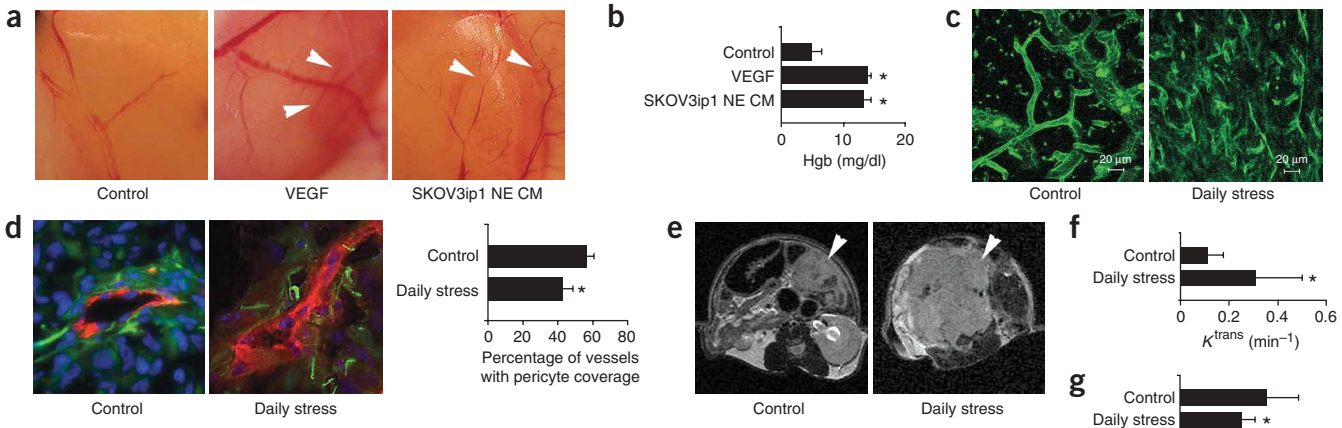

Figure 3 Effects of chronic stress on angiogenesis. (**a**) Representative images of Matrigel containing either serum-free SKOV3ip1 conditioned medium (control), VEGF (0.25 nM), or serum-free conditioned medium from norepinephrine-treated SKOV3ip1 cells (SKOV3ip1 NE CM). Newly formed blood vessels in the Matrigel are indicated by arrowheads. (**b**) We excised the Matrigel plugs and used them for quantification of angiogenesis by measuring the hemoglobin (Hgb) content in the Matrigel matrix. $^*P < 0.01$ versus control. (**c**) We visualized tumor vasculature from HeyA8 tumors in control and stressed animals by confocal fluorescence microscopy after perfusion with FITC-lectin. (**d**) We examined vessel maturation by determining the extent of pericyte coverage in tumors from control and chronic stress-exposed animals using triple immunofluorescence (CD31 (red) for endothelial cells, desmin (green) for pericytes and Hoechst (blue) for nuclei). $^*P < 0.01$. (**e**) Magnetic resonance imaging (MRI) was used to evaluate the functional characteristics of the tumor vasculature. Representative *in vivo* axial images of intraperitoneal HeyA8 ovarian tumors (arrowheads) from control and stressed animals were acquired in a 4.7-T scanner using a T2-weighted fast spin echo sequence (FSE) and respiratory gating (day 18 post-inoculation with HeyA8 cells). Vascular parameters derived from dynamic contrast–enhanced MRI included (**f**) K^{trans}, the volume transfer constant between blood plasma and extravascular extracellular space, (**g**) k_{ep}, the rate constant between extravascular extracellular space and blood plasma and (**h**) v_e, the volume of extravascular extracellular (interstitial) space per unit volume of tissue. We made measurements from the enhancing periphery of each tumor ($n = 8$ per group; $^*P < 0.05$). Error bars represent s.e.m.

extracellular space and blood plasma (k_{ep}, the return rate of contrast to plasma; **Fig. 3g**). In comparison, the volume of the extravascular extracellular space per unit volume of tissue (v_e) was greater in the stressed animals (**Fig. 3h**).

Given that behavioral stress induced significant anatomical and functional alterations in tumor vasculature, we sought to determine whether VEGF activity had a key role in mediating stress-induced acceleration in tumor growth. Stress effects on the number and weight of HeyA8 tumor nodules were completely blocked by co-administration of either the VEGF-R2 inhibitor PTK787 (50 mg/kg orally, daily) or the monoclonal VEGF-specific antibody bevacizumab (5 mg/kg intraperitoneally twice per week) (**Fig. 4a**,**b** and **Supplementary Fig. 7** online).

To more clearly define the mechanism by which β-adrenergic signaling regulates VEGF production, we examined transcriptional changes in activity of the *VEGF* gene after catecholamine stimulation. In SKOV3ip1 cells, *VEGF* mRNA expression increased by a peak 842% 1.5 h after exposure to norepinephrine (**Fig. 4c**), and promoter activity increased by 1,240% (**Fig. 4d**). This effect was blocked by propranolol, was mimicked by isoproterenol and was not observed in *ADRB*-negative A2780 ovarian cancer cells, implicating β-adrenoreceptors as a key mediator (**Fig. 4c** and data not shown). Subsequent studies showed that β-adrenergic stimulation modulates *VEGF* gene expression via the cAMP–protein kinase A (PKA) signaling pathway; the adenylyl cyclase activator forskolin (1 μM) and the PKA activator dibutyryl cAMP (db-cAMP; 1 mM) also stimulated

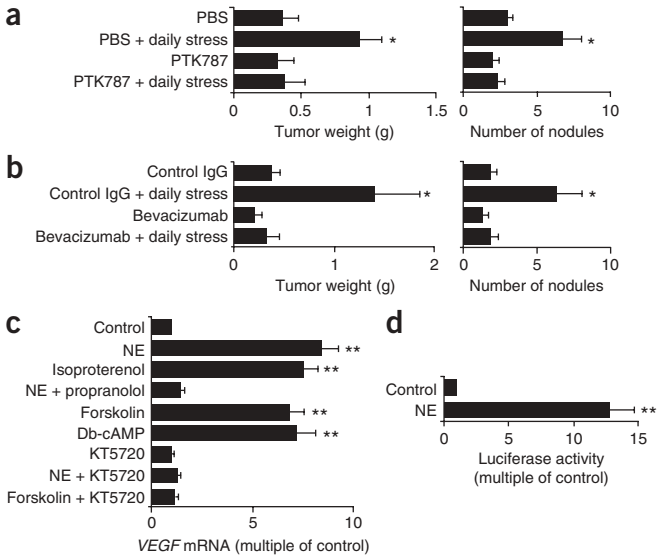

Figure 4 Effect of VEGF on stress-induced tumor growth. (**a**) HeyA8-injected mice were randomly assigned to one of the following four groups (4 d after tumor cell injection; $n = 10$ per group): control, oral placebo with stress, 50 mg/kg oral PTK787 (VEGF-R2 inhibitor) daily with no stress, or PTK787 with stress. (**b**) HeyA8-injected mice were randomly assigned to one of the following four groups (4 d after tumor cell injection; $n = 10$ per group): control, oral placebo with stress, bevacizumab (VEGF-specific antibody; 5 mg/kg intraperitoneally, twice per week) with no stress, or bevacizumab with stress. Treatment with PTK787 or bevacizumab blocked the stress-induced increase in tumor weight and number of nodules compared with treatment with the oral placebo (PBS) plus stress. (**c**) *VEGF* mRNA increased significantly when SKOV3ip1 cells were stimulated with norepinephrine (1 μM), isoproterenol (1 μM), forskolin (activator of cAMP) (1 μM), or dibutyryl cAMP (db-cAMP) (1 mM). KT5720 (1 μM) is a selective inhibitor of the cAMP-dependent protein kinase A and blocked VEGF induction by norepinephrine and forskolin. (**d**) In SKOV3ip1 cells, the VEGF promoter activity was increased by 1,280% after norepinephrine treatment compared with vehicle control. $^*P \leq 0.01$; $^{**}P \leq 0.001$.

VEGF mRNA (**Fig. 4c**), and the PKA inhibitor KT5720 could efficiently block *VEGF* mRNA induction by norepinephrine and forskolin (**Fig. 4c**).

Together, these results demonstrate a complete pathway by which behavioral stress can directly regulate the growth of ovarian carcinomas *in vivo*. Stress-induced release of catecholamines can activate *ADRB2* on ovarian carcinoma cells to trigger increased expression of the *VEGF* gene, which results in enhanced tumor vascularization and more aggressive growth and spread of malignant cells. In addition to providing the first experimental demonstration that behavioral stressors can enhance the pathogenesis of ovarian carcinoma *in vivo*, these data also suggest new approaches for adjuvant therapy in metastatic disease (for example, β-blockade).

The present study also expands our understanding of the general pathways by which stress can regulate cancer pathogenesis. Previous research emphasized the role of the immune system in mediating stress effects on tumor growth and metastasis[1,12,13], but the present results show that the neuroendocrine stress response can also directly affect the growth and activity of malignant tissue through hormone receptors expressed by tumor cells. Key to the demonstration of this direct effect on tumor cell biology is the use of a mouse host–human tumor hybrid model that provides opportunities for species-specific molecular manipulations that focally affect the tumor, such as the use of siRNA specific to human *ADRB1* and *ADRB2* and the comparison of human tumors positive for *ADRB* expression with those lacking *ADRB* expression. In addition to these tumor tissue-specific manipulations, we carried out several additional studies to ensure that generalized changes in host physiology (such as effects of the host cardiovascular or lymphatic systems) or direct effects on tumor cell proliferation are not responsible for the observed effects of stress on tumor growth (**Supplementary Fig. 8** online).

Pharmacologic and genetic manipulations identify β-adrenergic signaling as a central mediator of stress effects in the model of stress used here, but these findings do not rule out the possibility that other neuroendocrine signaling pathways might modulate tumor cell biology under other circumstances (for example, stress effects involving the hypothalamic-pituitary-adrenal/glucocorticoid axis[14] or inhibitory effects of dopamine on VEGF activity[15] and tumor growth[16]). To the extent that behavioral processes modulate the activity of multiple hormones via the central nervous system[17–19] and those hormones influence tumor cell biology[6,20], interventions targeting neuroendocrine function at the level of the central nervous system could represent new strategies for protecting individuals with cancer from the detrimental effects of stress biology on the progression of malignant disease.

METHODS

Cell lines and culture conditions. We grew the HeyA8, SKOV3ip1, A2780, RMG-II (from N. Ueno and H. Itamochi, M.D. Anderson Cancer Center) and MB-231 (from J. Price, M.D. Anderson Cancer Center) cancer cell lines as previously described[8].

Chronic stress model. We obtained 10- to 12-week-old female athymic nude mice from the US National Cancer Institute. All experiments were approved by the Institutional Animal Care and Use Committee of the M.D. Anderson Cancer Center. We used a restraint-stress procedure based on previous studies[21], using a new physical restraint system that we designed (**Supplementary Fig. 1**). For the social isolation model, we randomly assigned mice to be group housed ($n = 5$ per cage) or individually housed ($n = 1$ per cage). There was a wall and minimum distance of 24 inches between cages for the isolated mice. For both models, we injected the ovarian cancer cells intraperitoneally into mice 7 d after starting stress in all groups. We necropsied animals 21 d after tumor cell injection. For beta-blockade, we inserted the Alzet osmotic minipumps (DURECT) containing PBS or *s*-propranolol hydrochloride (Sigma; 2 mg/kg/d)[22,23] on the nape of neck 7 d before initiation of restraint stress.

Short interfering RNA (siRNA) preparation. We purchased siRNAs targeted against *ADRB1* (target sequence 5′-CCGATAGCAGGTGAACTCGAA-3′) or *ADRB2* (target sequence: 5′-CAGAGTGGATATCACGTGGAA-3′) from Qiagen and incorporated them into a neutral liposome (1,2-dioleoyl-*sn*-glycero-3-phosphatidylcholine (DOPC)), as previously described[10,24].

Inhibition of VEGF-R signaling. We blocked VEGF-R signaling using PTK787 (Novartis) daily[25]. We also used the monoclonal VEGF-specific antibody bevacizumab (Genentech) in separate experiments.

Real-time RT-PCR. We extracted total RNA (Trizol reagent; Invitrogen) and performed reverse transcription using an oligo(dT) primer and Moloney murine leukemia virus (M-MLV) reverse transcriptase (Life Technologies). After PCR amplification, we obtained quantitative values (we normalized each sample on the basis of its I8S content). We obtained the VEGF primers from Applied Biosystems (number HS00173626-m1).

Promoter analysis. We transiently transfected ovarian cancer cells (Invitrogen Lipofectamine 2000) with the VEGF promoter-reporter constructs (obtained from L. Ellis, M.D. Anderson Cancer Center) and determined luciferase activity in triplicate as previously described[26].

Immunohistochemistry. We stained paraffin sections for CD31 (1:800 dilution, Pharmingen), MMP-2 (1:500 dilution, Chemicon), MMP-9 (1:200 dilution, Calbiochem), VEGF (1:500 dilution, Santa Cruz Biotechnology) and bFGF (1:1,000 dilution, Sigma) at 4 °C (refs. 8,24). We exposed control samples to secondary antibody alone, and they did not show any nonspecific staining. Details for immunostaining fixed frozen sections for CD31 and desmin have been reported previously[8]. To quantify MVD, we examined ten random 0.159 mm^2 fields at 100× magnification for each tumor and counted the microvessels within those fields[8]. We evaluated the degree of pericyte coverage in five fields per tumor (200× magnification) as either absent or present (defined as covering >50% of the vessel). We then calculated, for each tumor, the average percentage of covered vessels relative to uncovered vessels.

***In vivo* angiogenesis assay with Matrigel.** We exposed SKOV3ip1 cells to serum-free medium with 1 μM of norepinephrine or vehicle for 24 h. We collected supernatants and centrifuged them to remove cells. We infused the conditioned medium with phenol-red free Matrigel (2:3 proportion, total 500 μl; BD Biosciences)[27]. We performed subcutaneous injections in mice for the three treatment groups ($n = 3$), and VEGF (0.25 nM) served as positive control. We killed the mice after 8 d and extracted the Matrigel plug for hemoglobin content (QuantiChrom hemoglobin assay; BioAssay Systems).

***In situ* hybridization.** We performed *in situ* hybridization for *VEGF* and analyzed results as described previously (**Supplementary Methods** online)[28].

Tumor vessel imaging. We anesthetized tumor-bearing mice and injected them intravenously with 100 μl of fluorescein *Lycopersicon esculentum* lectin (Vector Laboratories). Ten minutes later, we perfused mice through the ascending aorta with 4% paraformaldehyde for 2 min. Tumors were extracted, fixed, embedded in OCT, and sectioned for visualization using confocal fluorescence microscopy[29].

Magnetic resonance imaging. We performed all magnetic resonance imaging experiments using a 4.7-T Biospec small animal imaging system (Bruker Biospin USA). For anatomic tumor imaging, we used axial T2-weighted fast spin echo sequence (TE/TR 60 ms/1,050 ms; in-plane resolution 120 μm; slice thickness 1 mm; skip 0.25 mm; 3 nex) to delineate the tumor. For functional imaging, we acquired a series of axial, dynamic-contrast-enhanced images during and after contrast (diluted Magnevist) injection through a tail-vein catheter. We used an interleaved fast spoiled gradient echo sequence (TE/TR 1.4 ms/40 ms; in-plane resolution 312 mm × 234 mm; 1 mm slice thickness;

update rate 5.5 s per slice package) to monitor contrast accumulation in blood vessels and tumor. We analyzed regions of interest encompassing the enhancing periphery of the tumor. We measured functional tissue parameters by fitting contrast levels to a two-compartment pharmacokinetic model[30].

Assessment of tumor VEGF levels. We quantified concentrations of VEGF in tumor tissue homogenates using an ELISA kit (R&D Systems).

Statistical analysis. We compared continuous variables with either Student's *t*-test or analysis of variance (ANOVA) and compared categorical variables with χ^2. We used nonparametric tests (Mann-Whitney test), if appropriate, to compare differences. We considered $P < 0.05$ to be significant.

Note: Supplementary information is available on the Nature Medicine website.

ACKNOWLEDGMENTS

The authors thank I.J. Fidler, J. Price, C. Bucana, G. Gallick and A. Johnson for their helpful input and discussions regarding this work. We thank D. Reynolds for assistance with immunohistochemistry. We also thank J. Johnson and E. Schrock for assistance with manuscript preparation. This work was supported by US National Institutes of Health (NIH) grants (CA-11079301 and CA-10929801), the Donna Marie Cimitile-Fotheringham Award for Ovarian Cancer Research, the U.T. M.D. Anderson Ovarian Cancer SPORE (2P50 CA083639-06A1), and a Program Project Development Grant from the Ovarian Cancer Research Fund, Inc. to A.K.S., NIH grant CA-104825 to S.K.L., and NIH grant A152737 to S.W.C.

AUTHOR CONTRIBUTIONS

P.H.T., L.Y.H. and A.A.K. designed and performed experiments and wrote portions of the manuscript. J.M.A. and R.T. designed and performed VEGF transcription and promoter assays and edited the manuscript. C.L., N.B.J., G.A.-P., W.M.M., Y.G.L., M.L., L.S.M., T.J.K., C.N.L. and Y.L. designed and performed experiments and edited the manuscript. E.F. and R.A.N. designed and performed catecholamine analyses and edited the manuscript. J.A.B., M.R. and V.K. designed and performed the imaging experiments and edited the manuscript. A.M.S. and G.L.-B. performed siRNA incorporations and edited the manuscript. R.L.C. and D.M.G. performed statistical analyses and edited the manuscript. S.K.L., S.W.C. and A.K.S. designed the overall study, analyzed data and edited the manuscript.

COMPETING INTERESTS STATEMENT

The authors declare that they have no competing financial interests.

Published online at http://www.nature.com/naturemedicine/
Reprints and permissions information is available online at http://npg.nature.com/reprintsandpermissions/

1. Antoni, M.H. *et al.* The influence of bio-behavioural factors on tumour biology: pathways and mechanisms. *Nat. Rev. Cancer* **6**, 240–248 (2006).
2. Justice, A. Review of the effects of stress on cancer in laboratory animals: importance of time of stress application and type of tumor. *Psychol. Bull.* **98**, 108–138 (1985).
3. Ben-Eliyahu, S. The promotion of tumor metastasis by surgery and stress: immunological basis and implications for psychoneuroimmunology. *Brain Behav. Immun.* **17** (Suppl.), S27–S36 (2003).
4. Reiche, E.M., Nunes, S.O. & Morimoto, H.K. Stress, depression, the immune system, and cancer. *Lancet Oncol.* **5**, 617–625 (2004).
5. McEwen, B. Seminars in Medicine of the Beth Israel Deaconness Medical Center: protective and damaging effects of stress mediators. *N. Engl. J. Med.* **338**, 171–179 (1998).
6. Lutgendorf, S.K. *et al.* Vascular endothelial growth factor and social support in patients with ovarian carcinoma. *Cancer* **95**, 808–815 (2002).
7. Lutgendorf, S.K. *et al.* Stress-related mediators stimulate vascular endothelial growth factor secretion by two ovarian cancer cell lines. *Clin. Cancer Res.* **9**, 4514–4521 (2003).
8. Thaker, P.H. *et al.* Antivascular therapy for orthotopic human ovarian carcinoma through blockade of the vascular endothelial growth factor and epidermal growth factor receptors. *Clin. Cancer Res.* **11**, 4923–4933 (2005).
9. Paredes, A. *et al.* Stress promotes development of ovarian cysts in rats: the possible role of sympathetic nerve activation. *Endocrine* **8**, 309–315 (1998).
10. Landen, C.N. *et al.* Therapeutic EphA2 gene targeting in vivo using neutral liposomal small interfering RNA delivery. *Cancer Res.* **65**, 6910–6918 (2005).
11. Langley, R.R. *et al.* Tissue-specific microvascular endothelial cell lines from H-2K(b)-tsA58 mice for studies of angiogenesis and metastasis. *Cancer Res.* **63**, 2971–2976 (2003).
12. Glaser, R. & Kiecolt-Glaser, J.K. Stress-induced immune dysfunction: implications for health. *Nat. Rev. Immunol.* **5**, 243–251 (2005).
13. Lutgendorf, S. *et al.* Social support, psychological distress and natural killer cell activity in ovarian cancer. *J. Clin. Oncol.* **23**, 7105–7113 (2005).
14. Chrousos, G.P. & Gold, P.W. The concepts of stress and stress system disorders. Overview of physical and behavioral homeostasis. *J. Am. Med. Assoc.* **267**, 1244–1252 (1992).
15. Basu, S. *et al.* The neurotransmitter dopamine inhibits angiogenesis induced by vascular permeability factor/vascular endothelial growth factor. *Nat. Med.* **7**, 569–574 (2001).
16. Teunis, M.A. *et al.* Reduced tumor growth, experimental metastasis formation, and angiogenesis in rats with a hyperreactive dopaminergic system. *FASEB J.* **16**, 1465–1467 (2002).
17. Seeman, T.E., Berkman, L.F., Blazer, D. & Rowe, J.W. Social ties and support and neuroendocrine function: the McArthur studies of successful aging. *Ann. Behav. Med.* **16**, 95–106 (1994).
18. Turner-Cobb, J.M., Sephton, S.E., Koopman, C., Blake-Mortimer, J. & Spiegel, D. Social support and salivary cortisol in women with metastatic breast cancer. *Psychosom. Med.* **62**, 337–345 (2000).
19. Antoni, M.H. *et al.* Cognitive-behavioral stress management reduces distress and 24-hour urinary free cortisol output among symptomatic HIV-infected gay men. *Ann. Behav. Med.* **22**, 29–37 (2000).
20. Costanzo, E.S. *et al.* Psychosocial factors and interleukin-6 among women with advanced ovarian cancer. *Cancer* **104**, 305–313 (2005).
21. Sheridan, J.F. *et al.* Restraint stress differentially affects anti-viral cellular and humoral immune responses in mice. *J. Neuroimmunol.* **31**, 245–255 (1991).
22. Aarons, R.D. & Molinoff, P.B. Changes in the density of beta adrenergic receptors in rat lymphocytes, heart and lung after chronic treatment with propranolol. *J. Pharmacol. Exp. Ther.* **221**, 439–443 (1982).
23. Exton, M.S. *et al.* Behaviorally conditioned immunosuppression in the rat is regulated via noradrenaline and beta-adrenoceptors. *J. Neuroimmunol.* **131**, 21–30 (2002).
24. Halder, J. *et al.* Focal adhesion kinase targeting for therapy of ovarian carcinoma using in vivo siRNA delivery in neutral liposomes. *Clin. Cancer Res.* (in the press).
25. Xu, L. *et al.* Inhibition of malignant ascites and growth of human ovarian carcinoma by oral administration of a potent inhibitor of the vascular endothelial growth factor receptor tyrosine kinases. *Int. J. Oncol.* **16**, 445–454 (2000).
26. Reinmuth, N. *et al.* Induction of VEGF in perivascular cells defines a potential paracrine mechanism for endothelial cell survival. *FASEB J.* **15**, 1239–1241 (2001).
27. Passaniti, A. *et al.* A simple, quantitative method for assessing angiogenesis and antiangiogenic agents using reconstituted basement membrane, heparin, and fibroblast growth factor. *Lab. Invest.* **67**, 519–528 (1992).
28. Radinsky, R. *et al.* A rapid colorimetric in situ messenger RNA hybridization technique for analysis of epidermal growth factor receptor in paraffin-embedded surgical specimens of human colon carcinomas. *Cancer Res.* **53**, 937–943 (1993).
29. Hu, L. *et al.* Vascular endothelial growth factor trap combined with paclitaxel strikingly inhibits tumor and ascites, prolonging survival in a human ovarian cancer model. *Clin. Cancer Res.* **11**, 6966–6971 (2005).
30. Daldrup, H. *et al.* Correlation of dynamic contrast-enhanced MR imaging with histologic tumor grade: comparison of macromolecular and small-molecular contrast media. *AJR Am. J. Roentgenol.* **171**, 941–949 (1998).